Compact, spatial-mode-interaction-free, ultralow-loss, nonlinear photonic integrated circuits

(Student paper)

Xinru Ji[1], Junqiu Liu[1], Jijun He[1], Rui Ning Wang[1], Zheru Qiu[1], Johann Riemensberger[1] and Tobias J. Kippenberg[1]

[1] Institute of Physics, Swiss Federal Institute of Technology Lausanne (EPFL), CH-1015 Lausanne, Switzerland

* Email: xinru.ji@epfl.ch

We implement Euler bends to build compact high-Q $\mathrm{Si_3N_4}$ racetrack microresonators, featuring a small footprint of only 0.21 mm^2 for 19.8 GHz free spectral range. We demonstrate that these multi-mode microresonators can be operated in the single-mode regime and generate a single soliton microcomb.

Keywords: *Compact high-Q Si_3N_4 microresonator, single-mode operation*

INTRODUCTION

For Kerr nonlinear photonics, anomalous GVD is required, which is realized via geometric dispersion engineering using multi-mode waveguides. However, uncontrollable spatial mode coupling in highly over-moded waveguides is undesired, as it yields spectrally distributed avoided mode crossings (AMXs) with random strengths, prohibiting soliton formation [1] and significantly distorting soliton spectra [2].

Microring resonators are used to avoid mode mixing. Single solitons with repetition rates in the microwave X- and K-band are generated [3], however the devices suffer from significant footprints and constrained device density. Alternatively, mode filtering elements [5] can be used to suppress mode mixing, yet at the same time limit the Q-factor.

Here, we demonstrate single mode operation in multi-mode $\mathrm{Si_3N_4}$ racetrack microresonators with two symmetric Euler π-bends [6, 7], which have a curvature (k, the inverse of radius) varying linearly with its path length (s),

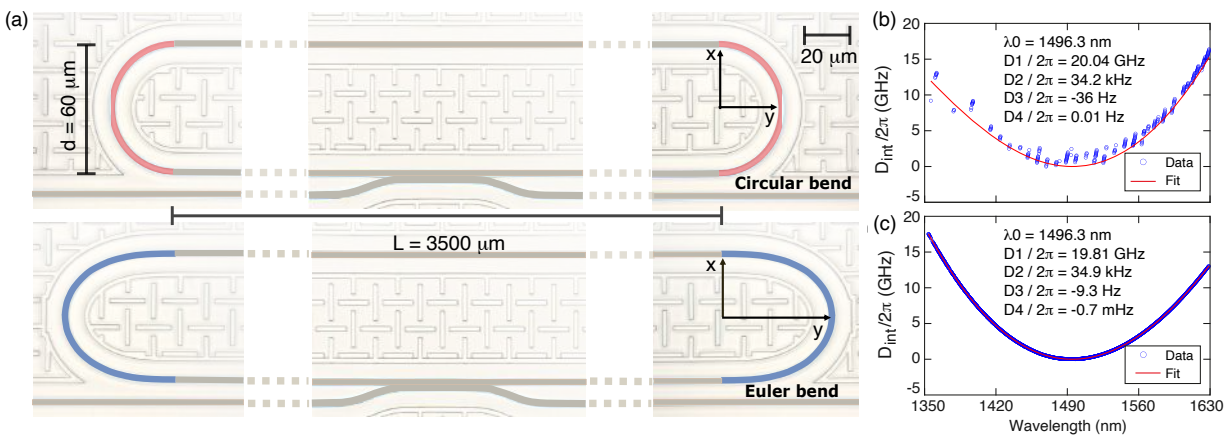

Fig. 1. Microscope image and integrated dispersion of Si_3N_4 racetrack microresonators with Euler bends and circular bends.

(a) Optical microscope images showing fabricated Si_3N_4 racetrack microresonators with Euler bends and circular bends. Both racetrack microresonators have the same span of d = 60 µm for the π-bends, and length of L = 3500 µm. The device footprint is approximately 0.21 mm^2. (b)-(c) Integrated dispersion characterization of racetrack microresonators with circular bends and Euler bends, fitted with $D_{int}(\mu) = D_2\,\mu^2/2 + D_3\,\mu^3/6 + D_4\,\mu^4/24$

i.e. k(s) = $\alpha \cdot$ s. The racetrack microresonators consist of two straight waveguides measuring L = 3500 μm in length, and two π-bends spanning d = 60 μm. The resulted footprint is only 0.21 mm^2 for 19.8 GHz free spectral range (FSR), which is considerably smaller than the footprint of microring resonators of the same FSR that cover an area of more than 4 mm^2 in Ref. [3]. Such a size reduction allows for the integration of 30 devices on a 5 × 5 mm^2 chip. It also benefits devices that have capacitance dependence on area, e.g, piezoelectric modulators [4], where a small footprint allows to reduce the time constant and increase the modulation speed.

RESULTS

We fabricated $\mathrm{Si_3N_4}$ racetrack microresonators using the photonic Damascene reflow process [8]. The $\mathrm{Si_3N_4}$ waveguide has a cross-section of 2.2 μm width and 0.90 μm height, featuring 10 transverse eigenmodes. To characterize resonance linewidths (i. e. microresonator loss) and microresonator dispersion, we use frequency-comb-assisted, cascaded diode laser spectroscopy, to cover the entire telecommunication E- to L-band (1350 to 1630 nm) [9]. We quantitatively characterize the strength of spatial mode interaction by studying the microresonator dispersion, and investigate AMXs. Figure 1(b,c) show the measured integrated microresonator dispersion with 4-th order fitting.

For the racetrack microresonator with Euler bends, AMXs are not observable in the dispersion profile. They are only revealed when D_2 and D_3 terms are both removed. While for the racetrack microresonator with circular bends, the missing resonances and exaggerated AMXs prohibit to fit D_{int} in Figure 1(c), leading to infeasibility to extract D_3

and D_4 values.

Finally, we demonstrate single soliton generation of 19.8 GHz repetition rate in the racetrack microresonator with

Euler bends. We observe a soliton step length of ~ 0.5 ms, on par with the previously reported value in a 100-GHz-FSR microresonator [10]. Due to the suppressed AMXs, the soliton step is sufficiently long, allowing for direct access to the single soliton state using simple laser piezo frequency tuning, without any other complex tuning schemes or auxiliary lasers. An erbium-doped fiber amplifier (EDFA) is used to increase the on-chip pump power to approximately 55.7 mW to seed soliton formation. Figure 2(a) shows the single soliton spectrum, which does not show prominent dispersive wave features caused by AMXs. The single soliton spectrum fit shows a 3-dB bandwidth of 16.3 nm, corresponding to a pulse duration of 156 fs.

Further single-sideband (SSB) phase noise measurement of the soliton repetition rate shows a weak quite point effect [11], indicating inhibited dispersive wave generation, due to suppressed spatial mode interaction and avoided- mode crossings.

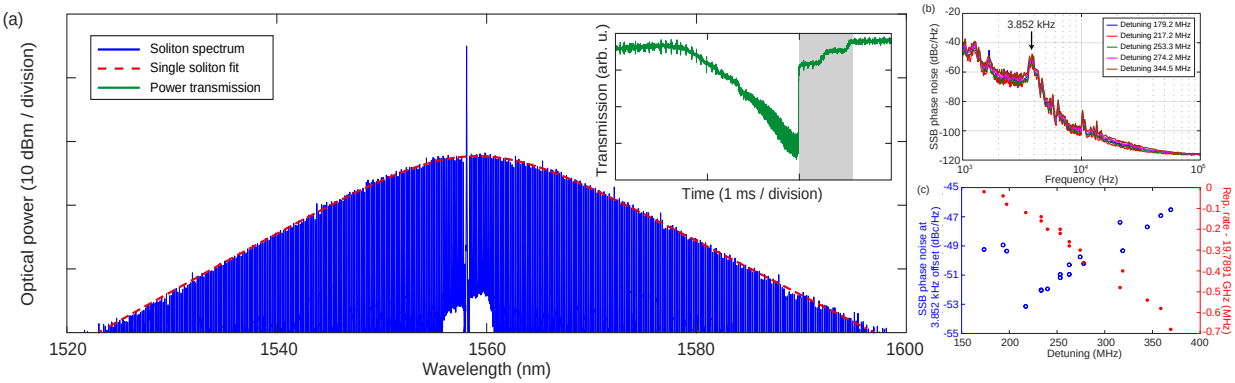

Fig. 2. Single soliton generation in the racetrack microresonator with Euler bends, and the phase noise characterization of soliton repetition rate. (a) Single soliton spectra of 19.8 GHz repetition rate. No prominent dispersive wave features caused by AMXs are observed. Inset: When the pump laser scans across the resonance, a soliton step of ~ 0.5 ms length in the microresonator transmission is seen (marked in the gray zoom). (b) SSB phase noise measurement with different soliton detuning values. No prominent phase noise change due to the quiet point operation is observed. The feature at 3.852 kHz Fourier offset frequency is caused by the diode laser pump [3]. (c) SSB phase noise at 3.852 kHz Fourier offset frequency and measured repetition rate shift with different soliton detuning values. The absence of strong quiet point is likely due to the inhibited dispersive wave generation that is caused by the suppressed spatial mode interaction and avoided-mode crossings.

Acknowledgements: This work was supported by the Air Force Office of Scientific Research (AFOSR) under Award No. FA9550-19-1-0250, by Contract HR0011- 20-2-0046 (NOVEL) from the Defense Advanced Research Projects Agency (DARPA), Microsystems Technology Office (MTO), by the Swiss National Science Foun- dation under grant agreement No. 176563 (BRIDGE), and by the EU H2020 research and innovation programme under grant agreement No. 965124 (FEMTOCHIP). The Si_3N_4 chips were fabricated in the EPFL center of MicroNanoTechnology (CMi).

References

[1] T. Herr *et al.,* Phys. Rev. Lett. 113, 123901 (2014)
[2] S. Ramelow *et al.,* Opt. Lett. 39, 5134 (2014)
[3] J. Liu *et al.,* Nat. Photonics 14, 486–491 (2020)
[4] J. Liu *et al.,* Nature 583, 385–390 (2020)
[5] A. Kordts *et al.*, Opt. Lett. 41, 452 (2016)
[6] T. Fujisawa *et al.,* Opt. Express 25, 9150 (2017)
[7] F. Vogelbacher *et al.,* Opt. Express 27, 31394 (2019)
[8] J. Liu *et al.,* Nature Communications 12, 2236 (2021)
[9] J. Liu *et al.,* Opt. Lett. 41, 3134 (2016).
[10] J. Liu *et al.,* Optica 5, 1347 (2018).
[11] Yi, X. *et al.,* Nat Commun 8, 14869 (2017)